Bioorganic Chemistry 91 (2019) 103131

Contents lists available at ScienceDirect

Bioorganic Chemistry

journal homepage: www.elsevier.com/locate/bioorg

Design, synthesis and biological evaluation of novel perimidine *o*-quinone derivatives as non-intercalative topoisomerase II catalytic inhibitors

Du-Chao Zhou, Yu-Ting Lu, Yan-Wen Mai, Chen Zhang, Jie Xia, Pei-Fen Yao, Hong-Gen Wang, Shi-Liang Huang*, Zhi-Shu Huang

School of Pharmaceutical Sciences, Sun Yat-sen University, Guangzhou 510006, People's Republic of China

ARTICLE INFO

Keywords:
Topoisomerase II
Anti-proliferation
Catalytic inhibitor
Perimidine *o*-quinone
Mansonone
Apoptosis

ABSTRACT

For the development of novel anticancer agents, we designed and synthesized a total of 37 perimidine *o*-quinone derivatives containing the *o*-quinone group at the A or B ring and different substituents (alkyl groups, aryl groups or heterocycles) at the C ring of the compounds. The structure-activity relationships (SARs) were established based on the cytotoxicity data of compounds from the HL-60, Huh7, Hct116, and Hela cell lines. The cytotoxicity results showed that most compounds exhibited potent cytotoxicity. In particular, compound **b-12** showed the best anti-proliferative activity ($IC_{50} \leq 1$ μM) against four cancer cell lines and strong potency against the HL-60/MX2 (0.47 μM) cell line, which is resistant to Topo II poisons. Further studies showed that **b-12** exhibited potent Topo IIα inhibitory activity ($IC_{50} = 7.54$ μM) compared with Topo I, which acted as a class of non-intercalative Topo IIα catalytic inhibitor by inhibiting the ATP binding site of Topo II. Cell apoptosis and cell cycle assays confirmed that **b-12** could induce the apoptosis of Huh7 cells in a dose-dependent manner.

1. Introduction

Human topoisomerase (Topo) has been regarded as an important target in anticancer drug discovery for more than 30 years. Topo can transiently interrupt one or both strands of DNA to solve the topology that arises in double-stranded DNA, which is crucial for the replication, transcription and other cellular transactions of DNA in cell life [1]. Numerous researchers have been focusing on the search for promising anticancer agents targeting at Topo II because of its high expression levels in proliferating cancer cells, which is essential to cancer cell survival.

On the basis of different mechanisms of action, Topo II-targeting agents could classified into two major classes, namely, "Topo II poisons" and "Topo II catalytic inhibitors". Poisons, such as etoposide (VP-16), are believed to stabilize the drug-Topo-DNA cleavable complexes and induce DNA breakage. Agents acting on any other steps in the catalytic cycle are called catalytic inhibitors [2]. For example, Topo II catalytic inhibitors interfere with the binding between DNA and Topo II (aclarubicin [3,4]), inhibit ATP binding (novobiocin), block DNA breakage (merbarone) [2], or hinder the ATP hydrolysis (ICR-187 and structurally related bisdioxopiperazine derivatives) [5]. To date, Topo II poisons, such as VP-16 and doxorubicin, have been extensively and effectively used in clinical oncology. However, these poisons present numerous side effects, such as frequent tumor recurrence and resistance, especially cardiotoxicity and secondary malignancies, which substantially limits their application [6,7]. Therefore, Topo II catalytic inhibitors are superior to Topo II poisons for clinical cancer therapy [2].

o-Quinone-containing compounds have attracted considerable research attention [8]. Compounds such as salvicine [9], β-lapachone [10], dunione and mansonone [11], all showed potent antitumor activity and strong Topo II inhibitory effects. The SARs confirmed the importance of the *o*-quinone moiety to the cytotoxicity against cancer cell lines of these compounds. Furthermore, the structure of perimidines leads to their consideration as potential antitumor compounds, and a large number of 2-substituted perimidines (**1, 2**) [12,13] and some other perimidine derivatives (**3**) [14] (Fig. 1), which all showed potent cytotoxicity against different cancer cell lines, have been designed and synthesized. However, the mechanism of action of these perimidine derivatives has yet to be elucidated.

In an effort to discover novel anticancer agents as non-intercalative Topo II catalytic inhibitors, 37 novel perimidine *o*-quinone derivatives were designed by the combination of the perimidine skeleton and *o*-quinone structure (Fig. 2). The synthesized compounds were evaluated for their antiproliferation against four cancer cell lines and inhibitory activity against Topo enzymes. DNA unwinding, Topo II cleavage, and ATP-dependent relaxing assays were carried out to investigate the inhibitory mechanisms of compound **b-12**.

* Corresponding author.
E-mail address: lsshsl@mail.sysu.edu.cn (S.-L. Huang).

https://doi.org/10.1016/j.bioorg.2019.103131
Received 8 May 2019; Received in revised form 18 July 2019; Accepted 18 July 2019
Available online 22 July 2019

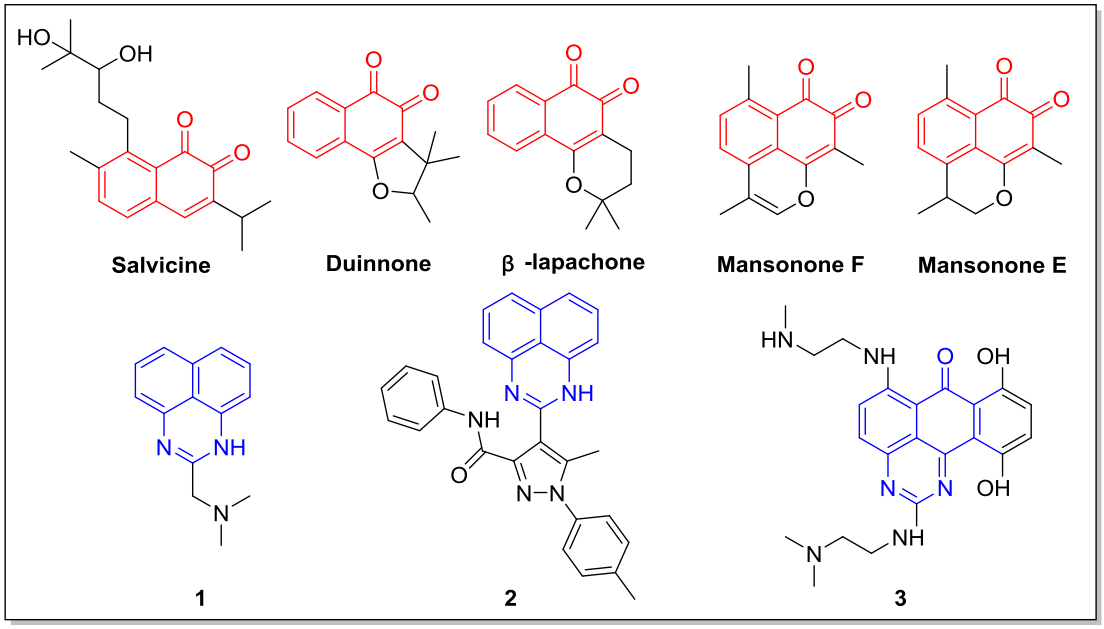

Fig. 1. The structures of *o*-quinone compounds and perimidine derivatives.

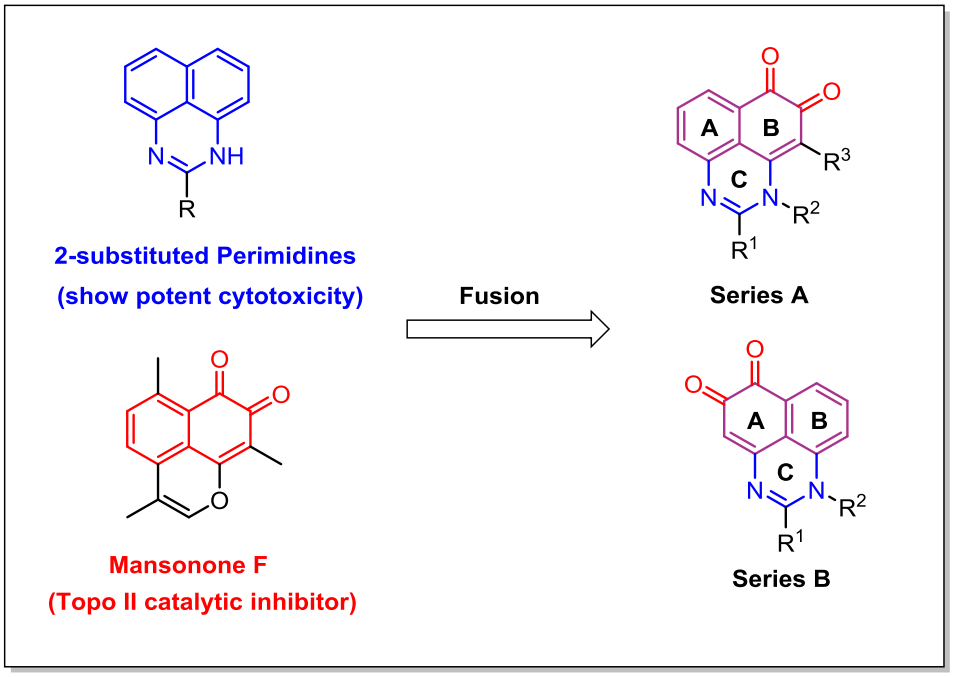

Fig. 2. Design of novel perimidine *o*-quinone agents as potential Topo II catalytic inhibitors.

2. Chemistry

In this study, 37 perimidine *o*-quinone derivatives (**a-1** to **a-17**, **b-1** to **b-17**, and **d-1** to **d-3**) were designed and synthesized, and the general structures are shown in Table 1. These compounds were prepared following the procedures described in Scheme 1. Intermediates **I** (**I-1** to **I-17**) were easily prepared in high yields by refluxing a mixture of sodium pyrosulfite, an aldehyde and 1,8-diaminonaphthalene in ethanol [15]. Then, intermediates **I** and CH_3I or CH_3CH_2I were reacted in DMF to give the methylated or ethylated products **II** (**II-1** to **II-17**). Intermediate **II** was subjected to $NaNO_2$ in the presence of acetic acid to yield two nitro intermediates **IIIa** (6-nitro substituent) and **IIIb** (7-nitro substituent), which were used without further purification. The nitro group of the two intermediates was reduced to the corresponding amines **IVa** and **IVb** and further oxidized by Fremy's salt to yield the two series isomers (series **A** and series **B**) of target products, which could be separated by column chromatography through a gradient elution using dichloromethane: methanol (100:1–50:1).

Furthermore, substitutions at the C-9 position of several series **B** derivatives were obtained by different methods. Chloro-substituted and bromo-substituted perimidine *o*-quinone derivatives were obtained by treatment with *N*-chlorosuccinimide and *N*-bromosuccinimide, respectively.

All new compounds were confirmed by chromatographic (HPLC) and spectroscopic (NMR and HRMS) methods. As an example, the additional HMQC and HMBC spectra of the compounds **a-1** and **b-1** were provided to prove the position of *o*-quinone group (SI file).

Table 1
IC_{50} values (μM) of perimidine *o*-quinone derivatives against cancer cells and inhibition rate (I.R.%) of Topo II.

Compd	R^1	R^2	R^3	IC_{50} (μM)[a]					Topo II I.R(%)[b] (5μM)
				HL-60	Huh7	Hct116	Hela	HL-60/MX2	
a-1	$-CH_3$	$-CH_3$	–	0.73 ± 0.11	0.80 ± 0.20	3.74 ± 0.33	2.27 ± 0.33	–	20
b-1	$-CH_3$	$-CH_3$	–	1.32 ± 0.31	9.14 ± 3.67	18.6 ± 4.00	14.7 ± 3.09	–	23
a-2	$-CH_2CH_3$	$-CH_3$	–	0.80 ± 0.18	1.93 ± 0.16	2.48 ± 0.87	1.34 ± 0.40	–	< 20
b-2	$-CH_2CH_3$	$-CH_3$	–	2.91 ± 0.12	3.87 ± 0.56	5.41 ± 0.76	7.67 ± 1.00	–	< 20
a-3		$-CH_3$	–	0.67 ± 0.11	3.87 ± 0.27	1.86 ± 0.30	4.32 ± 0.72	–	30
b-3		$-CH_3$	–	0.83 ± 0.11	5.45 ± 1.37	3.17 ± 1.00	6.15 ± 1.10	–	< 20
a-4	$-CH_2-C_6H_5$	$-CH_3$	–	0.84 ± 0.15	1.70 ± 0.17	3.14 ± 1.15	2.01 ± 0.48	–	54
b-4	$-CH_2-C_6H_5$	$-CH_3$	–	0.78 ± 0.09	0.81 ± 0.13	4.40 ± 0.42	1.63 ± 0.84	–	55
a-5	$-C_6H_5$	$-CH_3$	–	3.72 ± 0.29	1.13 ± 0.15	3.35 ± 0.63	1.88 ± 0.89	–	57
b-5	$-C_6H_5$	$-CH_3$	–	0.64 ± 0.09	1.20 ± 0.29	2.39 ± 0.20	1.45 ± 0.47	–	57
a-6	$4\text{-}CH_3C_6H_4-$	$-CH_3$	–	3.73 ± 0.49	1.81 ± 0.20	3.29 ± 0.84	5.01 ± 1.98	–	< 20
b-6	$4\text{-}CH_3C_6H_4-$	$-CH_3$	–	1.71 ± 0.16	2.78 ± 0.63	1.83 ± 0.30	3.06 ± 0.70	–	45
a-7	$4\text{-}OCH_3C_6H_4-$	$-CH_3$	–	1.23 ± 0.24	10.8 ± 2.65	6.24 ± 1.30	8.48 ± 1.53	–	< 20
b-7	$4\text{-}OCH_3C_6H_4-$	$-CH_3$	–	0.43 ± 0.06	2.30 ± 0.18	2.96 ± 0.77	3.28 ± 0.62	–	< 20
a-8		$-CH_3$	–	1.45 ± 0.32	5.89 ± 1.13	4.34 ± 1.27	6.59 ± 1.47	–	< 20
b-8		$-CH_3$	–	0.77 ± 0.15	2.71 ± 0.32	1.70 ± 0.60	14.13 ± 3.96	–	< 20
a-9	$2\text{-}ClC_6H_4-$	$-CH_3$	–	0.54 ± 0.13	2.54 ± 0.24	1.21 ± 0.08	2.99 ± 0.66	–	42
b-9	$2\text{-}ClC_6H_4-$	$-CH_3$	–	0.49 ± 0.09	3.01 ± 0.73	1.45 ± 0.82	2.58 ± 0.22	–	< 20
a-10	$2\text{-}ClC_6H_4-$	$-CH_2CH_3$	–	0.86 ± 0.07	1.85 ± 0.38	1.22 ± 0.27	3.00 ± 0.68	–	< 20
b-10	$2\text{-}ClC_6H_4-$	$-CH_2CH_3$	–	0.54 ± 0.11	1.03 ± 0.13	1.59 ± 0.43	1.41 ± 0.50	–	53
a-11	$3\text{-}ClC_6H_4-$	CH_3	–	0.87 ± 0.17	2.46 ± 0.47	1.56 ± 0.37	2.86 ± 0.63	–	38
b-11	$3\text{-}ClC_6H_4-$	CH_3	–	0.63 ± 0.10	2.47 ± 0.26	0.63 ± 0.20	1.52 ± 0.55	–	33
a-12	$4\text{-}ClC_6H_4-$	CH_3	–	1.30 ± 0.19	1.13 ± 0.11	2.18 ± 0.15	2.14 ± 0.21	–	50
b-12	$4\text{-}ClC_6H_4-$	CH_3	–	0.31 ± 0.08	0.45 ± 0.05	0.97 ± 0.20	1.08 ± 0.35	0.47 ± 0.08	60
a-13	$2\text{-}FC_6H_4-$	CH_3	–	1.12 ± 0.26	7.22 ± 1.80	4.34 ± 1.80	16.6 ± 4.16	–	52
b-13	$2\text{-}FC_6H_4-$	CH_3	–	0.36 ± 0.07	1.69 ± 0.15	2.39 ± 0.69	2.39 ± 0.35	–	36
a-14	$3\text{-}FC_6H_{54}-$	CH_3	–	1.18 ± 0.28	3.14 ± 0.85	2.35 ± 0.03	2.81 ± 0.64	–	39
b-14	$3\text{-}FC_6H_4-$	CH_3	–	0.41 ± 0.12	1.44 ± 0.14	1.46 ± 0.58	2.09 ± 0.88	–	51
a-15	$4\text{-}FC_6H_4-$	CH_3	–	2.58 ± 0.43	1.65 ± 0.27	1.20 ± 0.56	2.20 ± 0.78	–	< 20
b-15	$4\text{-}FC_6H_4-$	CH_3	–	1.01 ± 0.19	1.28 ± 0.32	1.78 ± 0.24	1.24 ± 0.24	–	31
a-16	$2,4\text{-di-}FC_6H_3-$	CH_3	–	0.69 ± 0.16	2.51 ± 0.41	0.96 ± 0.10	3.50 ± 1.15	–	32
b-16	$2,4\text{-di-}FC_6H_3-$	CH_3	–	0.47 ± 0.06	1.99 ± 0.60	1.38 ± 0.37	3.17 ± 1.27	–	32
a-17	$2,3,4\text{-tri-}FC_6H_2-$	CH_3	–	0.72 ± 0.16	3.48 ± 0.44	2.14 ± 0.48	4.77 ± 1.50	–	43
b-17	$2,3,4\text{-tri-}FC_6H_2-$	CH_3	–	0.36 ± 0.10	0.51 ± 0.15	0.43 ± 0.11	0.69 ± 0.17	0.93 ± 0.15	69
d-1	$2\text{-}ClC_6H_4-$	CH_3	−Br	0.71 ± 0.11	1.88 ± 0.21	1.04 ± 0.40	2.22 ± 0.68	–	54
d-2	$2\text{-}ClC_6H_4-$	CH_3	−Cl	3.27 ± 0.46	4.87 ± 0.38	2.90 ± 0.79	7.09 ± 1.47	–	37
d-3	$-CH_2CH_3$	CH_3	−Br	0.65 ± 0.06	6.59 ± 1.11	3.91 ± 0.70	5.97 ± 1.36	–	61
VP-16	–	–	–	0.52 ± 0.13	12.9 ± 1.92	13.5 ± 1.22	18.7 ± 5.17	10.3 ± 2.54	85

[a] The IC_{50} represents the compound concentration yielding 50% survival of each cell line after 48 h.
[b] The inhibition rate (I.R. %) is calculated base on optical density analysis of agarose gel electrophoretogram of the Topo II mediated DNA relaxation assay in the presence of different compounds (5 μM) and positive control VP-16 (200 μM) (Fig. S1 of SI file).

3. Results and discussion

3.1. In vitro cytotoxicity

The synthesized compounds were evaluated for their cytotoxicity against four tested cancer cell lines including HL-60, Huh7, Hct116 and Hela, by using the MTT assay. VP-16 was used as a positive control. The inhibitory activities (IC_{50}) of the tested compounds are shown in Table 1. As is evident from the IC_{50} values, most compounds showed stronger sensitivity against the suspended cell line (HL-60) than the attached cell lines (Huh7, Hct116, and Hela) and stronger cytotoxicity than the positive control (VP-16). Among them, compounds **b-12** and **b-17** showed the best anti-proliferation against the four cancer cell lines with IC_{50} values lower than 1 μM. To gain insight into involvement of Topo II inhibition in the cytotoxicity of **b-12** and **b-17**, we assessed the anti-proliferative activity by using the HL-60/MX2 cell line, which is resistant to mitoxantrone and shows altered catalytic activity and reduced levels of Topo II. HL-60/MX2 cells generally remain sensitive to Topo II catalytic inhibitors and show resistance to Topo II poisons. The MTT assay demonstrated that **b-12** and **b-17** retained activity in the HL-60/MX2 cell line. The IC_{50} values of **b-12** and **b-17** were less than 1 μM, and their resistance indices (HL-60/MX2/HL-60) were 1.5 and 2.6, respectively. However, the IC_{50} value of VP-16 was 0.52 μM for HL-60 and 10.3 μM for HL-60/MX2, so the resistance index (HL-60/MX2/HL-60) was 19.8. These results implied that our compounds were Topo II catalytic inhibitors.

3.2. SARs based on the cytotoxicity data

(1) When R^1 was substituted by an alkyl, the compounds possessing *o*-quinone at ring A (series A) showed better cytotoxicity than those substituted at ring B (series B). On the other hand, the compounds (**a-9**, **b-9**, **a-10**, and **b-10**) with the R^2 substituted by methyl or ethyl groups exhibited similar cytotoxicity.
(2) In general, most compounds displayed poor cytotoxicity activity when R^1 was replaced by an aryl moiety substituted with electron-donating group ($4\text{-}CH_3OC_6H_4$ and $4\text{-}CH_3C_6H_4$) and an electronically rich heterocyclic group (thiophene). By contrast, when R^1 was replaced by an aryl moiety substituted with electron-withdrawing group (chlorophenyl, and fluorophenyl), most of the compounds showed better cytotoxicity. Similarly, the SARs of the compounds in the Topo II inhibitory activity (except **b-6** and **a-15**) are similar to the rules obtained on the cell, and the compounds **b-12** and **b-17** are excellent in both enzyme inhibition and cytotoxicity.
(3) The cytotoxicity of series **B** compounds in the HL-60 cell line was better than that of the series **A** compounds. But this trend was not

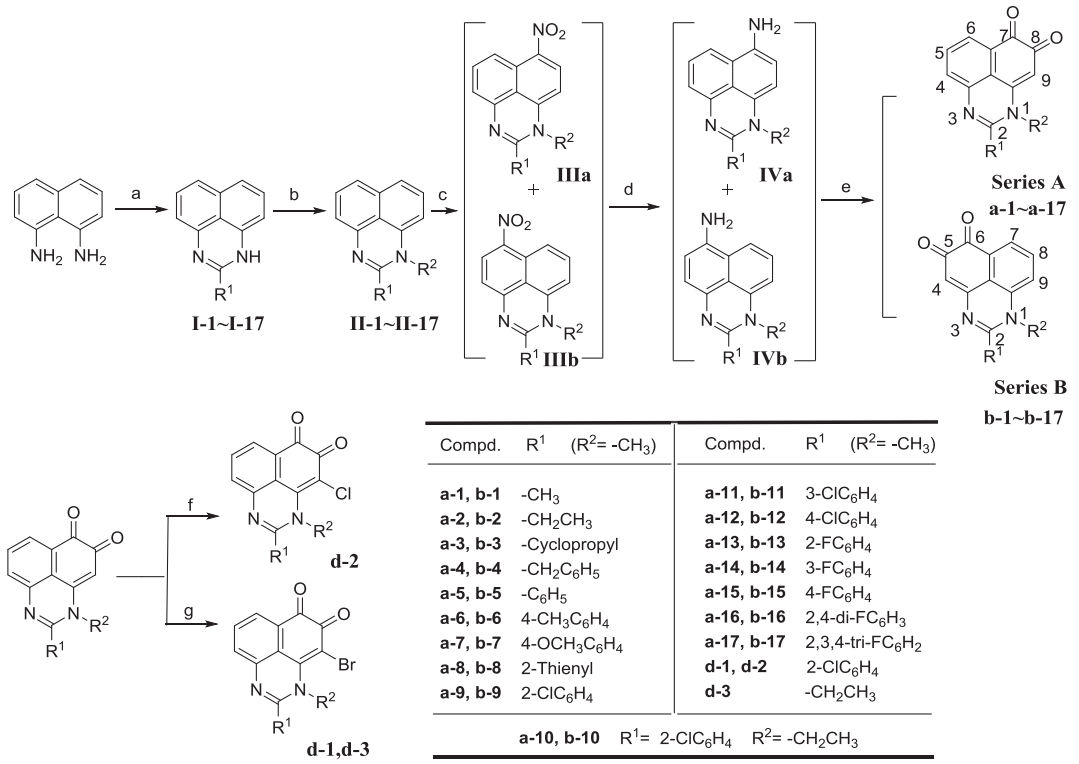

Compd.	R^1 (R^2= -CH_3)	Compd.	R^1 (R^2= -CH_3)
a-1, b-1	-CH_3	**a-11, b-11**	3-ClC_6H_4
a-2, b-2	-CH_2CH_3	**a-12, b-12**	4-ClC_6H_4
a-3, b-3	-Cyclopropyl	**a-13, b-13**	2-FC_6H_4
a-4, b-4	-$CH_2C_6H_5$	**a-14, b-14**	3-FC_6H_4
a-5, b-5	-C_6H_5	**a-15, b-15**	4-FC_6H_4
a-6, b-6	4-$CH_3C_6H_4$	**a-16, b-16**	2,4-di-FC_6H_3
a-7, b-7	4-$OCH_3C_6H_4$	**a-17, b-17**	2,3,4-tri-FC_6H_2
a-8, b-8	2-Thienyl	**d-1, d-2**	2-ClC_6H_4
a-9, b-9	2-ClC_6H_4	**d-3**	-CH_2CH_3
a-10, b-10	R^1= 2-ClC_6H_4	R^2= -CH_2CH_3	

Scheme 1. Reagents and conditions: (a) RCHO, $Na_2S_2O_5$, EtOH, reflux; (b) CH_3I or CH_3CH_2I, NaOH, DMF, 80 °C; (c) $NaNO_2$, AcOH, rt; (d) H_2, Pd/C, Ethyl acetate, 50 °C; (e) Acetone, 0.06 M KH_2PO_4, Fremy's salt, 10.4–44.4% (three-steps); (f) NCS, BPO, $CHCl_3$, 80 °C, 63%; (g) NBS, BPO, $CHCl_3$, 80 °C, 71–77.5%.

observed for the other three cell lines. Compounds **b-12** (R^1 = *p*-chlorophenyl) and **b-17** (R^1 = trifluorophenyl) showed the best anti-proliferative activity against the four cancer cell lines. However, unlike the SARs at the cellular level, there is no obvious rule for the inhibitory activity of the series **A** and series **B** compounds on the enzyme, which may be related to the complexity of the action of the compounds in the cell and specificity and selectivity of the compounds against Topo II.

(4) Furthermore, to investigate the effect of different substitutions at the C-9 position on the inhibitory activity of cancer cells, several chlorine or bromine replacement compounds were synthesized. Compounds (**d-1**, **d-2** and **d-3**) substituted at the C-9 position exhibited similar or weaker activity compared with the corresponding unsubstituted compounds (**a-9** and **a-2**).

3.3. Compound *b-12* As a Topo II inhibitor

The conversion of supercoiled plasmid DNA to relaxed DNA by Topo I and IIα in the presence of the prepared perimidine *o*-quinone derivatives (**b-12** and **b-17**) was evaluated as shown in Fig. 3.

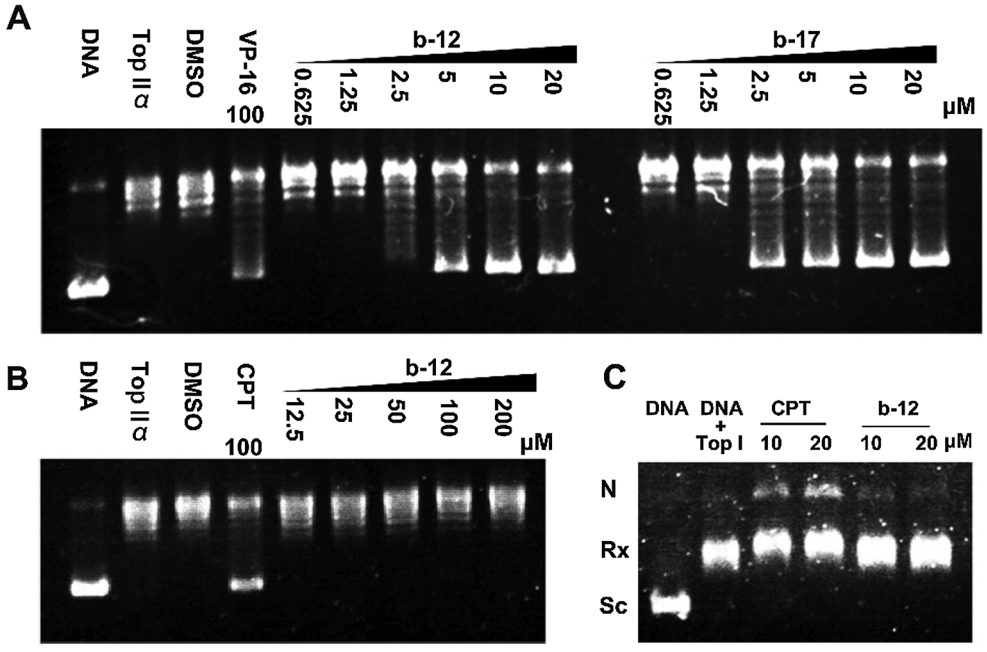

Fig. 3. (A) Topo IIα inhibitory activity of compounds **b-12** and **b-17** at different concentrations and VP-16 as a positive control. Supercoiled pBR322 plasmid was incubated with Topo IIα in the presence or absence of the indicated compounds at 37 °C for 30 min. (B) Topo I inhibitory activity of compound **b-12** at the concentrations of 200, 100, 50, 25, and 12.5 μM. Supercoiled pBR322 plasmid was incubated with Topo I in the presence or absence of the indicated compounds at 37 °C for 30 min. (C) Effect of **b-12** on the Topo I–DNA cleavage complex formation. Lanes 1 to 2: control group of supercoiled pBR322 without or with excess Topo I; Lanes 3 to 6: effect of CPT (10 and 20 μM) and **b-12** (10 and 20 μM) on excess Topo I with supercoiled pBR322. The positions of supercoiled DNA (Sc), relaxed DNA (Rx), and nicked DNA (N) are indicated.

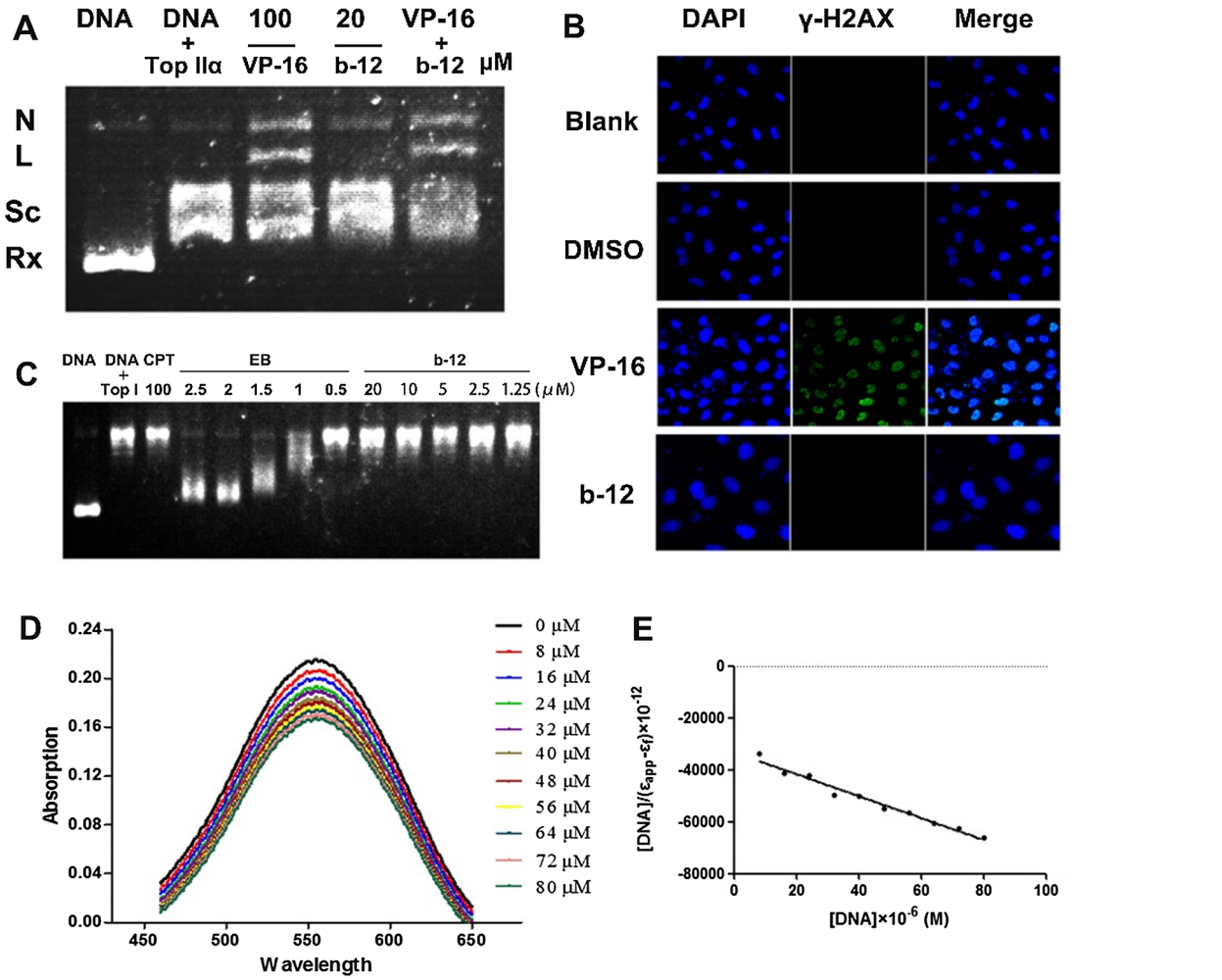

Fig. 4. (A) Effect of **b-12** on Topo II–DNA cleavage complex formation. Lanes 1 to 2: control group of supercoiled pBR322 without or with excess Topo II; Lanes 3 to 5: effect of VP-16 (100 μM), **b-12** (20 μM) and VP-16 (100 μM) and **b-12** (20 μM) together on excess Topo II with supercoiled pBR322. The positions of supercoiled DNA (Sc), relaxed DNA (Rx), linear DNA (L) and nicked DNA (N) are indicated. (B) Immunofluorescence assay. Images of blank (nontreated), DMSO, VP-16 (Topo II poison), and compound **b-12** in treated Huh7 cells. (C) The unwinding assay of **b-12**, where the positions of supercoil (Sc) and relax (Rx) DNA are indicated. (D) Absorption spectra of **b-12** upon addition of CT-DNA. [**b-12**] = 40 μM, [DNA] = 0–80 μM. The arrow indicates the absorption change upon increasing the amount of CT-DNA. (E) Insert graph shows the plot of [DNA]/(εa-εf) versus [DNA].

Camptothecin (CPT) and VP-16, respectively known as Topo I and Topo IIα inhibitors, were used as positive controls. The results (Fig. 3A) showed that **b-12** and **b-17** exhibited stronger Topo IIα inhibitory activity compared with the positive control. The IC_{50} values of the Topo IIα inhibition of **b-12** and **b-17** were 7.54 and 4.68 μM, respectively. However, in the Topo I relaxation and cleavage assay (Fig. 3B and C), compound **b-12** did not show Topo I inhibitory activity even at a high concentration, indicating that our compounds are a class of selective Topo II inhibitors. Because of the poor solubility of **b-17**, which will affect the follow-up experiment, **b-12** was selected as a candidate compound for further study.

3.4. Compound *b-12* As a non-Intercalative Topo II catalytic inhibitor

3.4.1. Compound b-12 As a Topo II catalytic inhibitor

Topo II poisons exhibit activity by stabilizing Topo II-DNA covalent complexes *in vitro* and *in vivo* and causing the formation of linear DNA [16,17]. As shown in Fig. 4A, VP-16 induced linear DNA formation at 100 μM. By contrast, **b-12** did not generate linear DNA at 20 μM. With VP-16 and **b-12** co-treatment, **b-12** did not markedly reduce the amount of linear DNA caused by VP-16, suggesting that **b-12** may act on the step after formation of Topo II-DNA complexes. γ-H_2AX is considered as a marker of DNA double-strand breaks (DSBs) [18], so the ability of **b-12** to induce DNA damage in the Huh7 cell line was also examined to confirm this mode of inhibition by immunofluorescence assay. The results (Fig. 4B) showed that VP-16 (20 μM) induced DNA DSBs, whereas **b-12** (2 μM) did not induce γ-H_2AX formation. These findings are consistent with the results obtained from the cleavage assay. The two experiments indicated that **b-12** may not be a Topo II poison but a catalytic inhibitor.

3.4.2. The binding properties between compound *b-12* and DNA

The unwinding effect is caused by certain compounds intercalating into the DNA, and the effect may yield false positive outcomes in the Topo-mediated DNA relaxation assay. Therefore, the DNA unwinding assay was performed using eukaryotic DNA (CT-DNA) with Topo I to identify whether compounds intercalate into the DNA. As shown in Fig. 4C, ethidium bromide (EB), a classic DNA intercalator, intercalated into the plasmid DNA by converting relaxed DNA to supercoiled DNA in a dose-dependent manner (0.5–2.5 μM) and was selected as a positive control. By contrast, compound **b-12** did not change the amount of supercoiled DNA even at a high concentration (20 μM) compared with the positive control. This finding provides evidence that **b-12** did not intercalate into DNA and is therefore not a DNA intercalator.

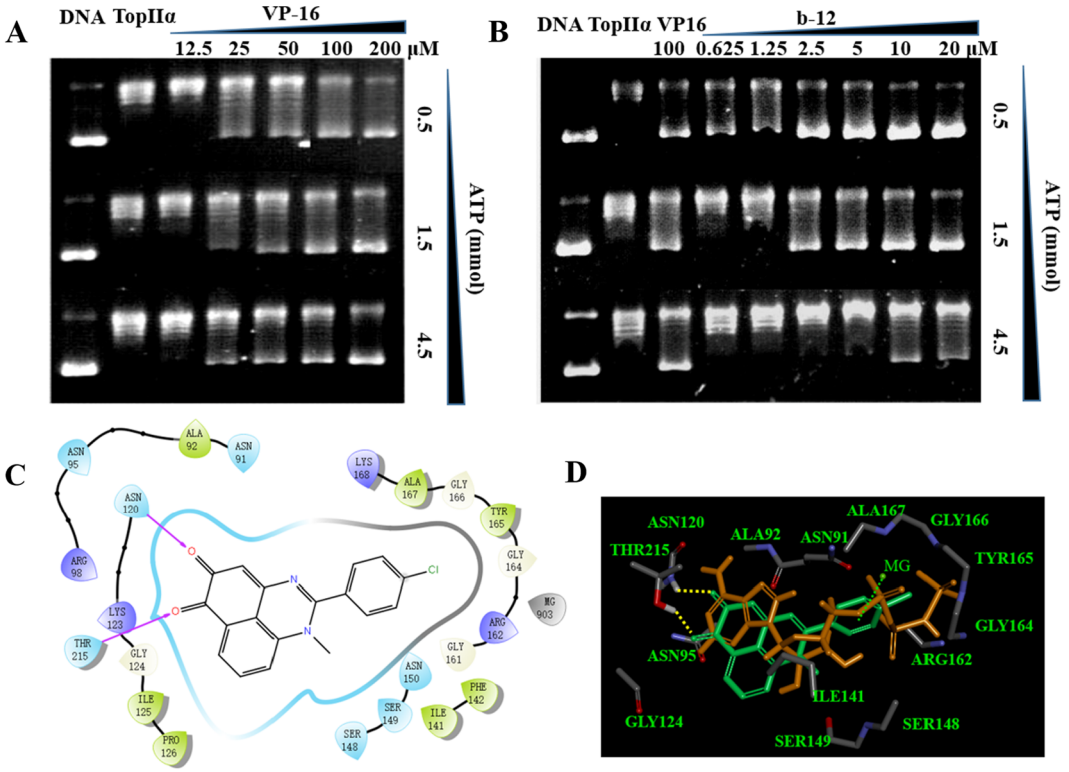

Fig. 5. (A) The effects of VP-16 on DNA relaxation catalyzed by Topo II at 37 °C for 30 min with 0.5 mM, 1.5 mM and 4.5 mM ATP. (B) The effects of **b-12** on DNA relaxation catalyzed by Topo II at 37 °C for 30 min with 0.5 mM, 1.5 mM and 4.5 mM ATP. (C) Interaction of compound **b-12** and the ATPase domain of topoisomerase IIα was displayed in the 2D diagram. (D) Overlay of compound **b-12** and ATP. The compound and the protein binding site are represented as sticks. Compound **b-12** and ATP are shown in green and pink, respectively.

In addition, a UV-titration assay was conducted to measure the binding ability of **b-12** to CT-DNA. If the compound intercalated into DNA, the UV curve of the compound would exhibit hypochromicity and bathochromic shift. In Fig. 4D, significant hypochromicity was not observed with increasing DNA concentration, and the analysis revealed that the binding constant (K_{app}) of **b-12** with DNA was $1.3 \times 10^4\ M^{-1}$. Taken together, these findings indicate that **b-12** is a nonintercalative Topo II catalytic inhibitor.

3.5. Compound *b-12* may target the ATPase of Topo II

To study the interaction between compounds and the ATPase domain of Topo II, we first conducted an ATP competitive assay. VP-16 is a Topo II poison that does not bind to the ATPase domain, so the inhibitory activity would not change with increasing ATP concentrations in Topo II-mediated DNA relaxation (Fig. 5A). The results of Fig. 5B showed that the inhibitory activity of **b-12** decreased with increasing ATP concentrations from 0.5 mM to 4.5 mM, and the corresponding inhibitory activity IC_{50} value for Topo II increased from approximately 2.5 μM to exceed 20 μM. These results revealed that **b-12** may act as an ATP competitive inhibitor by blocking the ATP-binding site of the enzyme.

Meanwhile, a docking study was carried out for compound **b-12** in the ATP-binding domain of human topoisomerase IIα [19] (PDB code: 1ZXM) by using Glide of Schrodinger. As seen from the images (Fig. 5C and D), the residues that are in close contact with **b-12** are Asn120, Thr215, Asn91, Asn95, Lys123, Gly124, Ile125, Ile141, Phe142, Ser149, Asn150, Ala167, and Lys168. Hydrogen bonding interaction occurs between the oxygen atoms of C6 and Asn120, C5 and Thr215, whereas the C-2 phenyl of compound **b-12** could form an interaction with Mg^{2+}. In addition, compound **b-12** and ATP could overlap well, and this finding could further explain that our compounds may target the ATPase domain of Topo IIα.

3.6. Compound *b-12* induces cell apoptosis

Apoptosis is the process of programmed cell death, which involves a series of biochemical events. We carried out cell apoptosis and cycle arrest assays to study the activity of **b-12** on the apoptosis of Huh7 cells. From the results (Fig. 6A) of the cell apoptosis assay, the percentage of apoptotic cells substantially increased in a dose-dependent manner, when cells were incubated with **b-12** (0.375, 0.5, 0.75, and 1 μM). DNA fragmentation could be caused by cell apoptosis, which is expressed as an apoptotic peak of Sub-G1 in the cell cycle assay. In Fig. 6B, the percentage of Sub-G1 phase evidently increased at a **b-12** concentration of 0.75 μM, whereas VP-16 could block the cell cycle in the G2/M phase. Topo II poisons can increase the level of DNA-enzyme-drug cleavage complexes. This DNA break can trigger recombination/repair pathways in G2 phase, thus showing G2/M phase arrest in cell cycle assay. However, Topo II catalytic inhibitor can stabilize DNA in the state of enzyme locking and block the cleavage/replication cycle of DNA, are not able to untangle daughter chromosomes and ultimately die of mitotic failure [20]. So compound **b-12** is no obvious effect on specificity of cell cycle. Taken together, all the results suggested that our compounds suppressed Huh7 cell proliferation by inducing apoptosis.

4. Conclusion

A series of novel perimidine *o*-quinone derivatives was designed, synthesized and evaluated for cytotoxicity against four human cancer cell lines. MTT assays showed that most prepared compounds exhibited potent cytotoxicity, and the SARs showed that the substitution of an electron-withdrawing group (chlorophenyl or fluorophenyl) on the C-2 position and the location of *o*-quinone in ring A or ring B were critical for the anti-proliferative activity of cancer cells. Among these compounds, **b-12** showed the best cytotoxicity against several cancer cell

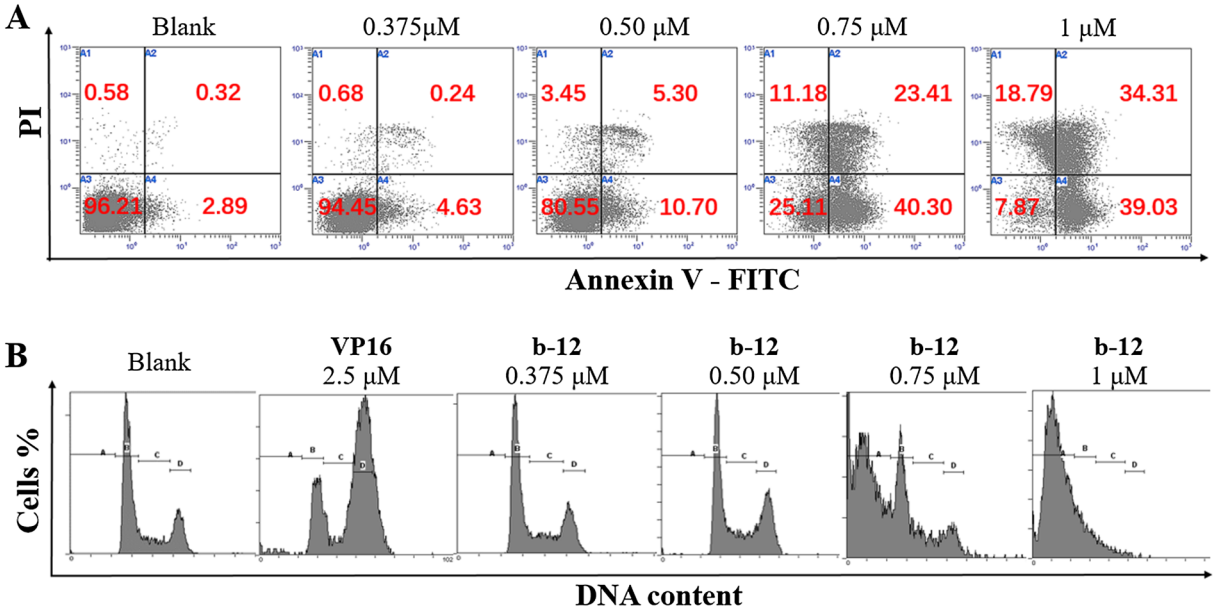

Fig. 6. (A) Apoptotic cells were detected with Fluorescein isothiocyanate (FITC) Annexin V/propidium iodide (PI) double staining after incubation of Huh7 cell with compound **b-12** for 24 h. (B) Cell arrest of Huh7 cell treated with **b-12** for 24 h.

lines and strong potency against the HL-60/MX2 (0.47 μM) cell line, which is resistant to Topo II poisons. Moreover, **b-12** showed good Topo IIα inhibitory activity (IC_{50} = 7.54 μM). Further mechanistic studies indicated that **b-12** was a non-intercalative Topo IIα catalytic inhibitor. The ATP competitive assay and docking study revealed that **b-12** may target the ATP binding site of Topo II. The cell apoptosis assay and cell cycle assay confirmed that **b-12** showed strong anti-proliferation against Huh7 cells by inducing apoptosis in a dose- dependent manner.

The present results indicate that perimidine *o*-quinone derivatives are potential novel anticancer agents. Given that Topo II is an important target for cancer chemotherapy, these findings may provide advanced opportunities for the design and development of new chemotherapy agents.

5. Experimental section

5.1. General

Compounds used as starting materials and reagents were from aladdin, innochem or other chemical companies and used without further purification. ^{1}HNMR, ^{13}CNMR, HMBC or HMQC spectra were recorded using TMS as the internal standard in $CDCl_3$ or DMSO-d_6 with a Bruker BioSpin GmbH spectrometer at 400 MHz. High resolution mass spectra (HRMS) were recorded on Shimadzu LCMS-IT-TOF. HPLC analysis showed that the purity of all the compounds was proved to be more than 95% by using analytical HPLC.

5.2. Procedure for the preparation of intermediate I

Sodium pyrosulfite (10 mmol) was dissolved in water (20 mL), 1,8-diaminonaphthalene (20 mmol) was dissolved in ethanol (100 mL) and the aldehyde (10 mmol) were successively added. The mixture was heated under reflux for 4 h. After completion of the reaction, the reaction mixture was warmed to room temperature and poured into the ice water. Solid would appear and filter, then the filtrate was used without further purification.

5.3. Procedure for the preparation of intermediate II

Intermediate **I** (10 mmol) and NaOH (20 mmol) were dissolved in dry DMF, CH_3I or CH_3CH_2I (15 mmol) was successively added. The reaction mixture was stirred at 80 °C for 4 h in the pressure tube. After completion of the reaction, the mixture was extracted with ethyl acetate, washed with saturated salt water for three times and concentrated to provide black yellow oil product, which were used for further purification with column chromatography to give the product. The ^{1}H NMR spectra of **II-1** to **II-17** were shown in SI.

5.4. Procedure for the preparation of targeted compounds (*a-1 ~ a-17, b-1 ~ b-17*)

Firstly, above intermediate **II** (10 mmol) and $NaNO_2$ (10 mmol) were dissolved in 15 mL acetic acid, which was stirred in the room temperature for 30 min. The reaction solution changed quickly from yellow to red and detected by TLC. Then the reaction mixture was concentrated directly by using rotary evaporator to give the red intermediate **III** without further purification. Then, a solution of intermediate **III** (20 mmol) in ethyl acetate (30 mL) was added to Pd/C (2 mmol), which was stirred at 50 °C in an atmosphere of H_2 until the reaction solution changed from red to yellow. After the reaction was completed, ethyl acetate was evaporated, then the product (intermediate **IV**) was used for next step without further purification. Finally, the intermediate **IV** (1 mmol) was dissolved in acetone (60 mL) and a solution of Fremy's salt (2.5 mmol) in 0.06-M KH_2PO_4 solution (40 mL) was added with vigorous stirring. After stirring for 30 min, the mixture was extracted by using chloroform with three times. The combined extracts were washed with saturated salt water (three times), dried over Na_2SO_4, filtered and evaporated to dryness. The solid residue was purified to give a pair of isomers (purple and red solid).

1,2-Dimethyl-1*H*-perimidine-7,8-dione (**a-1**): Red solid, Yield 24%. ^{1}H NMR (400 MHz, DMSO-d_6) δ 7.97 (dd, J = 5.4, 3.2 Hz, 1H), 7.80–7.74 (m, 2H), 5.84 (s, 1H), 3.52 (s, 3H), 2.60 (s, 3H). ^{13}C NMR (101 MHz, DMSO-d_6) δ 180.7, 177.2, 155.8, 151.7, 142.3, 134.3, 133.6, 129.7, 129.6, 117.9, 99.8, 36.6, 24.1. HRMS (ESI): calcd for $C_{13}H_{10}N_2O_2$ $[M+H]^+$ 227.0815, found 227.0809. HPLC purity: 99.6%.

1,2-Dimethyl-1*H*-perimidine-5,6-dione (**b-1**): Purple solid, Yield 21%. ^{1}H NMR (400 MHz, DMSO-d_6) δ 7.99 (d, J = 8.5 Hz, 1H), 7.94 (d, J = 7.3 Hz, 1H), 7.82 (t, J = 8.0 Hz, 1H), 5.74 (s, 1H), 3.74 (s, 3H), 2.58 (s, 3H). ^{13}C NMR (101 MHz, DMSO-d_6) δ 182.0, 177.8, 160.4, 158.1, 137.7, 133.7, 130.0, 128.3, 123.6, 116.5, 108.9, 35.8, 24.4.

HRMS (ESI): calcd for $C_{13}H_{10}N_2O_2$ $[M+H]^+$ 227.0815, found 227.0811. HPLC purity: 99.1%.

2-Ethyl-1-methyl-1*H*-perimidine-7,8-dione (**a-2**): Red solid, Yield 27%. ^{1}H NMR (400 MHz, DMSO-d_6) δ 7.97 (dd, J = 6.3, 2.3 Hz, 1H), 7.84–7.73 (m, 2H), 5.84 (s, 1H), 3.51 (s, 3H), 2.92 (q, J = 7.2 Hz, 2H), 1.27 (t, J = 7.3 Hz, 3H). ^{13}C NMR (101 MHz, DMSO-d_6) δ 180.7, 177.2, 158.6, 151.9, 142.1, 134.5, 133.6, 129.6, 129.6, 117.8, 99.8, 35.7, 28.6, 11.2. HRMS (ESI): calcd for $C_{14}H_{12}N_2O_2$ $[M+Na]^+$ 241.0947, found 241.0944. HPLC purity: 99.5%.

2-Ethyl-1-methyl-1*H*-perimidine-5,6-dione (**b-2**): Purple solid, Yield 23.5%. ^{1}H NMR (400 MHz, DMSO) δ 7.98 (dd, J = 19.9, 8.0 Hz, 2H), 7.85–7.80 (m, 1H), 5.77 (s, 1H), 3.75 (s, 3H), 2.89 (q, J = 7.4 Hz, 2H), 1.25 (t, J = 7.3 Hz, 3H). ^{13}C NMR (101 MHz, DMSO) δ 182.0, 177.8, 163.3, 158.1, 137.9, 133.7, 130.0, 128.4, 123.7, 116.4, 109.2, 35.1, 29.0, 11.3. HRMS (ESI): calcd for $C_{14}H_{12}N_2O_2$ $[M+H]^+$ 241.0966, found 241.0972. HPLC purity: 98.2%.

2-Cyclopropyl-1-methyl-1*H*-perimidine-7,8-dione (**a-3**): Red solid, Yield 10.4%. ^{1}H NM R (400 MHz, DMSO) δ 7.95 (dd, J = 6.9, 1.5 Hz, 1H), 7.80–7.69 (m, 2H), 5.87 (s, 1H), 3.72 (s, 3H), 2.32 (m, 1H), 1.18–1.02 (m, 4H). ^{13}C NMR (101 MHz, $CDCl_3$) δ 180.5, 177.7, 156.9, 152.2, 142.1, 134.4, 133.0, 130.2, 129.4, 117.7, 99.8, 35.4, 15.1, 8.6 (2C). HRMS (ESI): calcd for $C_{15}H_{12}N_2O_2$ $[M+H]^+$ 253.0972, found 253.0970. HPLC purity: 100%.

2-Cyclopropyl-1-methyl-1*H*-perimidine-5,6-dione (**b-3**): Purple solid, Yield 16.4%. ^{1}H NMR (400 MHz, DMSO) δ 8.00 (d, J = 8.5 Hz, 1H), 7.93 (d, J = 7.3 Hz, 1H), 7.82 (t, J = 8.0 Hz, 1H), 5.68 (s, 1H), 3.92 (s, 3H), 2.34 (d, J = 4.7 Hz, 1H), 1.47–1.01 (m, 4H). ^{13}C NMR (101 MHz, DMSO) δ 182.1, 177.5, 163.1, 158.1, 138.0, 133.7, 129.9, 128.1, 123.6, 116.4, 108.8, 35.3, 14.7, 10.2 (2C). HRMS (ESI): calcd for $C_{15}H_{12}N_2O_2$ $[M+H]^+$ 253.0972, found 253.0975. HPLC purity: 99.6%.

2-Benzyl-1-methyl-1*H*-perimidine-7,8-dione (**a-4**): Red solid, Yield 28%. m.p. 173.3- ^{1}H NMR (400 MHz, DMSO) δ 8.03 (dd, J = 7.0, 1.5 Hz, 1H), 7.86 (dd, J = 8.1, 1.5 Hz, 1H), 7.84–7.79 (m, 1H), 7.41–7.22 (m, 5H), 5.84 (s, 1H), 4.35 (s, 2H), 3.44 (s, 3H). ^{13}C NMR (101 MHz, $CDCl_3$) δ 180.2, 177.7, 154.9, 152.1, 141.8, 134.7, 134.3, 133.2, 130.8, 129.5, 129.4 (2C), 128.1 (2C), 127.8, 118.2, 100.0, 43.0, 36.1. HRMS (ESI): calcd for $C_{19}H_{14}N_2O_2$ $[M+H]^+$ 303.1128, found 303.1128. HPLC purity: 97.9%.

2-Benzyl-1-methyl-1*H*-perimidine-5,6-dione (**b-4**): Purple solid, Yield 26%. ^{1}H NMR (400 MHz, DMSO) δ 7.94 (d, J = 7.4 Hz, 2H), 7.88–7.78 (m, 1H), 7.32 (d, J = 26.5 Hz, 5H), 5.81 (s, 1H), 4.30 (s, 2H), 3.68 (s, 3H). ^{13}C NMR (101 MHz, DMSO) δ 181.7, 178.0, 160.9, 157.7, 137.9, 135.8, 133.7, 130.1, 129.3 (2C), 129.0 (2C), 128.6, 127.5, 123.8, 116.7, 109.6, 42.1, 35.9. HRMS (ESI): calcd for $C_{19}H_{14}N_2O_2$ $[M+H]^+$ 303.1128, found 303.1120. HPLC purity: 95.9%.

1-Methyl-2-phenyl-1*H*-perimidine-7,8-dione (**a-5**):Red solid, Yield 41.4%. ^{1}H NMR (400 MHz, $CDCl_3$) δ 8.24 (dd, J = 7.4, 1.0 Hz, 1H), 7.89 (dd, J = 8.1, 0.9 Hz, 1H), 7.74 (t, J = 7.8 Hz, 1H), 7.66–7.56 (m, 5H), 5.96 (s, 1H), 3.50 (s, 3H). ^{13}C NMR (101 MHz, $CDCl_3$) δ 179.1, 176.8, 154.9, 151.1, 140.9, 133.9, 133.4, 132.3, 129.9, 129.8, 128.4, 128.2 (2C), 127.2 (2C), 117.0, 99.5, 38.0. HRMS (ESI): calcd for $C_{18}H_{12}N_2O_2$ $[M+H]^+$ 289.0972, found 289.0974. HPLC purity: 99.1%.

1-Methyl-2-phenyl-1*H*-perimidine-7,8-dione (**b-5**):Purple solid, Yield 44.4%. ^{1}H NMR (400 MHz, DMSO) δ 8.02 (d, J = 7.9 Hz, 2H), 7.96–7.84 (m, 1H), 7.71 (d, J = 5.9 Hz, 2H), 7.59 (d, J = 6.9 Hz, 3H), 5.84 (s, 1H), 3.63 (s, 3H). ^{13}C NMR (101 MHz, DMSO) δ 181.6, 178.0, 160.1, 157.6, 138.1, 135.2, 133.9, 131.1, 129.9, 129.3 (2C), 129.0 (2C), 128.9, 124.5, 116.8, 109.9, 38.7. HRMS (ESI): calcd for $C_{18}H_{12}N_2O_2$ $[M+H]^+$ 289.0972, found 289.0966. HPLC purity: 98.0%.

1-Methyl-2-(*p*-tolyl)-1*H*-perimidine-7,8-dione (**a-6**): Red solid, Yield 30%. ^{1}H NMR (400 MHz, DMSO) δ 8.04 (dd, J = 7.1, 1.3 Hz, 1H), 7.85 (dd, J = 8.1, 1.3 Hz, 1H), 7.83–7.78 (m, 1H), 7.57 (d, J = 8.0 Hz, 2H), 7.36 (d, J = 7.9 Hz, 2H), 5.86 (s, 1H), 3.39 (s, 3H), 2.39 (s, 3H). ^{13}C NMR (101 MHz, $CDCl_3$) δ 180.2, 177.8, 156.2, 152.2, 142.0, 141.3, 135.0, 133.3, 131.5, 130.8, 129.8 (2C), 129.4, 128.2 (2C), 118.0, 100.5, 39.1, 21.5. HRMS (ESI): calcd for $C_{19}H_{14}N_2O_2$ $[M+H]^+$ 303.1128 found 303.1122. HPLC purity: 99.3%.

1-Methyl-2-(*p*-tolyl)-1*H*-perimidine-5,6-dione (**b-6**): Purple solid, Yield 29%. ^{1}H NMR (400 MHz, DMSO) δ 8.01 (d, J = 7.9 Hz, 2H), 7.9–7.86 (t, J = 8 Hz 1H), 7.61 (d, J = 8.1 Hz, 2H), 7.39 (d, J = 8.0 Hz, 2H), 5.82 (s, 1H), 3.65 (s, 3H), 2.42 (s, 3H). ^{13}C NMR (101 MHz, $CDCl_3$) δ 181.0, 178.3, 160.2, 157.3, 141.6, 137.5, 133.4, 131.4, 129.7 (3C), 128.9, 128.8 (2C), 122.4, 117.1, 111.4, 38.2, 21.6. HRMS (ESI): calcd for $C_{19}H_{14}N_2O_2$ $[M+H]^+$ 303.1128, found 303.1121. HPLC purity: 99.9%.

2-(4-Methoxyphenyl)-1-methyl-1*H*-perimidine-7,8-dione (**a-7**): Red solid, Yield 32.9%. ^{1}H NMR (400 MHz, DMSO) δ 8.05 (d, J = 7.0 Hz, 1H), 7.87 (d, J = 7.1 Hz, 1H), 7.85–7.80 (m, 1H), 7.67 (d, J = 8.6 Hz, 2H), 7.12 (d, J = 8.6 Hz, 2H), 5.88 (s, 1H), 3.86 (s, 3H), 3.45 (s, 3H). ^{13}C NMR (101 MHz, $CDCl_3$) δ 180.2, 177.8, 161.5, 155.9, 152.4, 142.1, 134.8, 133.2, 130.6, 130.1 (2C), 129.4, 126.6, 117.8, 114.5 (2C), 100.5, 55.6, 39.3. HRMS (ESI): calcd for $C_{19}H_{14}N_2O_3$ $[M+H]^+$ 319.1077, found 319.1073. HPLC purity: 99.6%.

2-(4-Methoxyphenyl)-1-methyl-1*H*-perimidine-5,6-dione (**b-7**): Purple solid, Yield 25.7%. ^{1}H NMR (400 MHz, DMSO) δ 8.02 (d, J = 7.9 Hz, 2H), 7.89 (dd, J = 8.6, 7.3 Hz, 1H), 7.76–7.66 (m, 2H), 7.15–7.10 (m, 2H), 5.84 (s, 1H), 3.86 (s, 3H), 3.69 (s, 3H). ^{13}C NMR (101 MHz, DMSO) δ 181.9, 177.9, 161.6, 160.1, 157.8, 138.5, 133.8, 131.6 (2C), 129.9, 128.7, 127.1, 124.5, 116.8, 114.4 (2C), 109.7, 56.0, 39.1. HRMS (ESI): calcd for $C_{19}H_{14}N_2O_3$ $[M+H]^+$ 319.1077, found 319.1075. HPLC purity: 99.6%.

1-Methyl-2-(thiophen-2-yl)-1*H*-perimidine-7,8-dione (**a-8**): Red solid, Yield 14.4%. ^{1}H NMR (400 MHz, $CDCl_3$) δ 8.19 (d, J = 7.3 Hz, 1H), 7.84 (d, J = 8.1 Hz, 1H), 7.71 (t, J = 7.7 Hz, 1H), 7.63 (d, J = 4.8 Hz, 1H), 7.53 (d, J = 2.7 Hz, 1H), 7.24–7.18 (m, 1H), 5.97 (s, 1H), 3.73 (s, 3H). ^{13}C NMR (101 MHz, $CDCl_3$) δ 180.1, 177.9, 152.5, 150.1, 141.9, 135.7, 134.9, 133.3, 131.0, 130.5, 130.3, 129.4, 127.7, 117.8, 100.9, 39.4. HRMS (ESI): calcd for $C_{16}H_{10}N_2O_2S$ $[M+H]^+$ 295.0536, found 295.0534. HPLC purity: 99.1%.

1-Methyl-2-(thiophen-2-yl)-1*H*-perimidine-5,6-dione (**b-8**): Purple solid, Yield 12.4%. ^{1}H NMR (400 MHz, DMSO) δ 8.02 (dd, J = 8, 4 Hz, 3H), 7.86 (t, J = 7.2 Hz, 2H), 7.31 (s, 1H), 5.82 (s, 1H), 3.94 (s, 3H). ^{13}C NMR (101 MHz, DMSO) δ 181.7, 177.8, 157.3, 154.1, 138.6, 137.0, 133.9, 133.7, 133.4, 129.9, 128.7, 128.7, 124.6, 116.8, 109.5, 38.8. HRMS (ESI): calcd for $C_{16}H_{10}N_2O_2S$ $[M+H]^+$ 295.0536, found 295.0531. HPLC purity: 99.7%.

2-(2-Chlorophenyl)-1-methyl-1*H*-perimidine-7,8-dione (**a-9**): Red solid, Yield 32%. ^{1}H NMR (400 MHz, $CDCl_3$) δ 8.27 (dd, J = 7.4, 1.2 Hz, 1H), 7.88 (dd, J = 8.1, 1.2 Hz, 1H), 7.80–7.73 (t, J = 7.6 Hz, 1H), 7.62–7.43 (m, 4H), 5.95 (s, 1H), 3.39 (s, 3H). ^{13}C NMR (101 MHz, $CDCl_3$) δ 180.0, 177.8, 153.5, 151.3, 141.8, 135.0, 133.8, 133.3, 132.4, 131.9, 131.2, 130.1, 130.0, 129.6, 128.1, 118.4, 100.4, 36.9. HRMS (ESI): calcd for $C_{18}H_{11}ClN_2O_2$ $[M+H]^+$ 323.0582, found 323.0575. HPLC purity: 97.8%.

2-(2-Chlorophenyl)-1-methyl-1*H*-perimidine-5,6-dione (**b-9**): Purple solid, Yield 34%. ^{1}H NMR (400 MHz, $CDCl_3$) δ 8.12 (d, J = 7.4 Hz, 1H), 7.75–7.70 (t, J = 8.4 Hz, 1H), 7.63 (dd, J = 5.9, 3.0 Hz, 1H), 7.58 (d, J = 8.4 Hz, 1H), 7.55–7.47 (m, 3H), 6.16 (s, 1H), 3.55 (s, 3H). ^{13}C NMR (101 MHz, DMSO) δ 181.2, 178.3, 157.4, 157.1, 137.3, 134.3, 134.1, 132.4, 131.2, 130.6, 130.2, 130.1, 129.3, 128.5, 124.2, 117.0, 110.4, 36.7. HRMS (ESI): calcd for $C_{18}H_{11}ClN_2O_2$ $[M+H]^+$ 323.0582, found 323.0575. HPLC purity: 97.6%.

2-(2-Chlorophenyl)-1-ethyl-1*H*-perimidine-7,8-dione (**a-10**): Red solid, Yield 29%. ^{1}H NMR (400 MHz, $CDCl_3$) δ 8.24 (d, J = 7.4 Hz, 1H), 7.85 (d, J = 8.1 Hz, 1H), 7.74 (t, J = 7.8 Hz, 1H), 7.62–7.42 (m, 4H), 5.98 (s, 1H), 3.92 (m, 1H), 3.78 (m, 1H), 1.26 (t, J = 7.1 Hz, 3H). ^{13}C NMR (101 MHz, $CDCl_3$) δ 180.1, 177.9, 153.2, 150.2, 141.8, 135.0, 133.8, 133.4, 132.3, 131.8, 131.4, 130.2, 129.9, 129.5, 127.7, 118.6, 100.5, 44.3, 12.1. HRMS (ESI): calcd for $C_{19}H_{13}ClN_2O_2$ $[M+H]^+$ 337.0738, found 337.0735. HPLC purity: 99.9%.

2-(2-Chlorophenyl)-1-ethyl-1*H*-perimidine-5,6-dione (**b-10**): Purple solid, Yield 22%. ^{1}H NMR (400 MHz, DMSO) δ 8.09 (d, J = 8.6 Hz, 1H),

8.05 (d, J = 7.4 Hz, 1H), 7.89 (t, J = 7.6 Hz, 1H), 7.77 (dd, J = 7.4, 1.6 Hz, 1H), 7.71 (d, J = 8.0 Hz, 1H), 7.67–7.52 (m, 2H), 5.85 (s, 1H), 4.21 (m, 1H), 3.82 (m, 1H), 1.19 (t, J = 7.1 Hz, 3H). ^{13}C NMR (101 MHz, DMSO) δ 181.2, 178.3, 157.0 (2C), 136.0, 134.2, 134.2, 132.3, 131.0, 130.6, 130.2, 130.2, 129.4, 128.4, 124.1, 117.3, 110.4, 44.0, 14.2. HRMS (ESI): calcd for $C_{19}H_{13}ClN_2O_2$ $[M+H]^+$ 337.0738, found 337.0731. HPLC purity: 97.5%.

2-(3-Chlorophenyl)-1-methyl-1*H*-perimidine-7,8-dione (**a-11**): Red solid, Yield 36%. ^{1}H NMR (400 MHz, $CDCl_3$) δ 8.26 (dd, J = 7.4, 1.2 Hz, 1H), 7.87 (dd, J = 8.1, 1.2 Hz, 1H), 7.79–7.73 (t, J = 8 Hz 1H), 7.62 (t, J = 1.6 Hz, 1H), 7.59–7.55 (m, 1H), 7.52 (t, J = 7.7 Hz, 1H), 7.47 (m, 1H), 5.95 (s, 1H), 3.49 (s, 3H). ^{13}C NMR (101 MHz, $CDCl_3$) δ 179.9, 177.8, 154.5, 151.8, 141.7, 136.0, 135.5, 134.9, 133.4, 131.1, 131.0, 130.5, 129.5, 128.5, 126.4, 118.2, 100.7, 38.9. HRMS (ESI): calcd for $C_{18}H_{11}ClN_2O_2$ $[M+H]^+$ 323.0582, found 323.0577. HPLC purity: 99.8%.

2-(3-Chlorophenyl)-1-methyl-1*H*-perimidine-5,6-dione (**b-11**): Purple solid, Yield 31%. ^{1}H NMR (400 MHz, DMSO) δ 8.08–7.96 (m, 2H), 7.87 (m, 1H), 7.77 (s, 1H), 7.65 (d, J = 7.3 Hz, 2H), 7.58 (dd, J = 8.8, 6.6 Hz, 1H), 5.83 (s, 1H), 3.59 (s, 3H). ^{13}C NMR (101 MHz, $CDCl_3$) δ 181.0, 179.0, 157.3, 156.7, 137.0, 134.0, 133.3, 132.2, 132.0, 130.4, 130.2, 130.1, 129.6, 128.2, 121.9, 117.9, 112.4, 36.1. HRMS (ESI): calcd for $C_{18}H_{11}ClN_2O_2$ $[M+H]^+$ 323.0582, found 323.0575. HPLC purity: 100%.

2-(4-Chlorophenyl)-1-methyl-1*H*-perimidine-7,8-dione (**a-12**): Red solid, Yield 14%. ^{1}H NMR (400 MHz, DMSO) δ 8.06 (dd, J = 7.2, 1.3 Hz, 1H), 7.88 (dd, J = 8.1, 1.3 Hz, 1H), 7.86–7.81 (m, 1H), 7.77–7.73 (m, 2H), 7.68–7.63 (m, 2H), 5.89 (s, 1H), 3.39 (s, 3H). ^{13}C NMR (101 MHz, $CDCl_3$) δ 180.0, 177.9, 154.9, 152.0, 141.8, 137.2, 135.0, 133.4, 132.8, 131.1, 129.8 (2C), 129.6 (2C), 129.4, 118.1, 100.7, 39.0. HRMS (ESI): calcd for $C_{18}H_{11}ClN_2O_2$ $[M+H]^+$ 323.0582, found 323.0576. HPLC purity: 100%.

2-(4-Chlorophenyl)-1-methyl-1*H*-perimidine-5,6-dione (**b-12**): Purple solid, Yield 28%. ^{1}H NMR (400 MHz, DMSO) δ 8.02 (d, J = 7.9 Hz, 2H), 7.94–7.82 (m, 1H), 7.75 (d, J = 8.6 Hz, 2H), 7.66 (d, J = 8.6 Hz, 2H), 5.84 (s, 1H), 3.62 (s, 3H). ^{13}C NMR (101 MHz, DMSO) δ 181.6, 178.1, 159.2, 157.5, 138.1, 135.9, 134.0, 133.9, 131.4 (2C), 129.9, 129.1 (2C), 129.0, 124.5, 116.9, 110.0, 38.7. HRMS (ESI): calcd for $C_{18}H_{11}ClN_2O_2$ $[M+H]^+$ 323.0588, found 323.0582. HPLC purity: 95.2%.

2-(2-Fluorophenyl)-1-methyl-1*H*-perimidine-7,8-dione (**a-13**): Red solid, Yield 18%. ^{1}H NMR (400 MHz, DMSO) δ 8.10 (dd, J = 7.1, 1.5 Hz, 1H), 7.91 (dd, J = 8.1, 1.5 Hz, 1H), 7.89–7.84 (t, J = 6.8 Hz 1H), 7.70 (m, 2H), 7.51–7.42 (m, 2H), 5.92 (s, 1H), 3.38 (d, J = 1.3 Hz, 3H). ^{13}C NMR (101 MHz, $CDCl_3$) δ 180.0, 177.8, 159.3 (d, J = 249.8 Hz), 151.7, 151.5, 141.9, 135.0, 133.1 (d, J = 8.2 Hz), 133.0, 131.2, 130.7 (d, J = 1.8 Hz), 129.6, 125.5 (d, J = 3.3 Hz), 122.6 (d, J = 15.1 Hz), 118.3, 116.2 (d, J = 20.6 Hz), 100.5, 37.5 (d, J = 2.7 Hz). HRMS (ESI): calcd for $C_{18}H_{11}FN_2O_2$ $[M+H]^+$ 307.0877, found 307.0869. HPLC purity: 95.6%.

2-(2-Fluorophenyl)-1-methyl-1*H*-perimidine-5,6-dione (**b-13**): Purple solid, Yield 22%. ^{1}H NMR (400 MHz, DMSO) δ 8.04–7.97 (m, 2H), 7.86 (dd, J = 8.6, 7.4 Hz, 1H), 7.73–7.59 (m, 2H), 7.50–7.30 (m, 2H), 5.82 (s, 1H), 3.56 (d, J = 1.4 Hz, 3H). ^{13}C NMR (101 MHz, DMSO) δ 181.3, 178.3, 158.9 (d, J = 247.8 Hz), 157.2, 155.6, 137.6, 134.0, 133.5 (d, J = 8.3 Hz), 131.3 (d, J = 1.8 Hz), 130.1, 129.3, 125.7 (d, J = 3.2 Hz), 124.3, 123.1 (d, J = 15.0 Hz), 117.0, 116.5 (d, J = 20.6 Hz), 110.3, 37.5 (d, J = 1.7 Hz). HRMS (ESI): calcd for $C_{18}H_{11}FN_2O_2$ $[M+H]^+$ 307.0877, found 307.0874. HPLC purity: 99.7%.

2-(3-Fluorophenyl)-1-methyl-1*H*-perimidine-7,8-dione (**a-14**): Red solid, Yield 19%. ^{1}H NMR (400 MHz, DMSO) δ 8.12–8.04 (m, 1H), 7.94–7.83 (m, 3H), 7.76–7.65 (m, 2H), 7.52–7.37 (m, 2H), 5.92 (s, 1H), 3.38 (s, 3H). ^{13}C NMR (101 MHz, $CDCl_3$) δ 180.0, 177.9, 159.3 (d, J = 250.0 Hz), 151.7, 151.5, 141.9, 133.1 (d, J = 8.3 Hz), 133.1, 133.0, 131.2, 130.6 (d, J = 1.8 Hz), 129.6, 125.5 (d, J = 3.2 Hz), 124.0 (d, J = 3.4 Hz), 118.4, 116.2 (d, J = 20.5 Hz), 100.5, 37.5 (d, J = 2.8 Hz). HRMS (ESI): calcd for $C_{18}H_{11}FN_2O_2$ $[M+H]^+$ 307.0877, found 307.0871. HPLC purity: 99.7%.

2-(3-Fluorophenyl)-1-methyl-1*H*-perimidine-5,6-dione (**b-14**): Purple solid, Yield 26.1%. ^{1}H NMR (400 MHz, DMSO) δ 8.03 (dd, J = 8, 3.6 Hz, 2H), 7.89 (dd, J = 16.1, 7.5 Hz, 1H), 7.79–7.74 (m, 2H), 7.41 (t, J = 8.4 Hz, 2H), 5.88 (s, 1H), 3.39 (s, 3H). HRMS (ESI): calcd for $C_{18}H_{11}FN_2O_2$ $[M+H]^+$ 307.0877, found 307.0872. HPLC purity: 98.8%.

2-(4-Fluorophenyl)-1-methyl-1*H*-perimidine-7,8-dione (**a-15**): Red solid, Yield 26.1%. ^{1}H NMR (400 MHz, DMSO) δ 8.07 (d, J = 6.8 Hz, 1H), 7.89 (d, J = 7.5 Hz, 1H), 7.87–7.81 (d, J = 7.6 Hz 1H), 7.81–7.76 (t, J = 7.6 Hz 1H), 7.43 (t, J = 8.4 Hz, 2H), 5.90 (s, 1H), 3.41 (s, 2H). ^{13}C NMR (101 MHz, $CDCl_3$) δ 180.0, 177.8, 164.0 (d, J = 252.6 Hz), 155.1, 152.0, 141.8, 134.9 (2C), 133.3 (2C), 130.8 (d, J = 8.1 Hz), 130.6, 130.5 (d, J = 3.6 Hz), 129.4, 118.0, 116.5 (d, J = 22.1 Hz), 100.7, 39.0. HRMS (ESI): calcd for $C_{18}H_{11}FN_2O_2$ $[M+H]^+$ 307.0877, found 307.0872. HPLC purity: 98.8%.

2-(4-Fluorophenyl)-1-methyl-1*H*-perimidine-5,6-dione (**b-15**): Purple solid, Yield 21%. ^{1}H NMR (400 MHz, DMSO) δ 8.03 (d, J = 7.9 Hz, 2H), 7.89 (t, J = 7.6 Hz, 1H), 7.82–7.77 (m, 2H), 7.43 (t, J = 8.9 Hz, 2H), 5.85 (s, 1H), 3.63 (s, 3H). ^{13}C NMR (101 MHz, DMSO) δ 181.7, 178.1, 163.7 (d, J = 248.2 Hz), 159.3, 157.5, 138.2 (2C), 133.9, 132.1 (d, J = 8.8 Hz), 131.7 (d, J = 3.0 Hz), 130.0 (2C), 129.0, 124.5, 116.9, 116.1 (d, J = 22.1 Hz), 109.9, 38.8. HRMS (ESI): calcd for $C_{18}H_{11}FN_2O_2$ $[M+H]^+$ 307.0877, found 307.0871. HPLC purity: 96.7%.

2-(2,4-Difluorophenyl)-1-methyl-1*H*-perimidine-7,8-dione (**a-16**): Red solid, Yield 19.3%. ^{1}H NMR (400 MHz, $CDCl_3$) δ 8.30–8.20 (d, J = 8.4, Hz 1H), 7.86 (d, J = 8.1 Hz, 1H), 7.75 (t, J = 7.8 Hz, 1H), 7.65 (m, 1H), 7.14 (m, 1H), 7.08–6.95 (m, 1H), 5.95 (s, 1H), 3.47 (d, J = 2.1 Hz, 3H). ^{13}C NMR (101 MHz, $CDCl_3$) δ 179.9, 177.8, 164.7 (dd, J = 255.4, 11.9 Hz), 159.8 (dd, J = 252.5, 12.4 Hz), 151.5, 150.9, 141.8, 135.0, 133.4, 132.1 (dd, J = 10.1, 4.0 Hz), 131.3, 129.5, 119.0 (dd, J = 15.6, 4.0 Hz), 118.3, 113.1 (dd, J = 21.8, 3.4 Hz), 104.8 (t, J = 25.3 Hz), 100.7, 37.6 (d, J = 3.1 Hz). HRMS (ESI): calcd for $C_{18}H_{10}F_2N_2O_2$ $[M+H]^+$ 325.0783, found 325.0781. HPLC purity: 100%.

2-(2,4-Difluorophenyl)-1-methyl-1*H*-perimidine-5,6-dione (**b-16**): Purple solid, Yield 17.4%. ^{1}H NMR (400 MHz, $CDCl_3$) δ 8.06 (d, J = 7.4 Hz, 1H), 7.78 (m, 1H), 7.75–7.69 (t, J = 8.4 Hz 1H), 7.58 (d, J = 8.4 Hz, 1H), 7.14 (m, 1H), 7.04–6.94 (m, 1H), 6.07 (s, 1H), 3.65 (d, J = 2.3 Hz, 3H). ^{13}C NMR (101 MHz, DMSO) δ 180.2, 177.2, 163.1 (dd, J = 250.6, 12.3 Hz), 158.4 (dd, J = 250.4, 12.9 Hz), 156.0, 153.8, 136.5, 132.9, 131.9 (dd, J = 10.4, 3.7 Hz), 129.0, 128.3, 123.3, 118.7 (dd, J = 15.3, 3.9 Hz), 115.9, 112.0 (dd, J = 22, 3.3 Hz), 109.2, 104.2 (t, J = 25.9 Hz), 36.5 (d, J = 1.9 Hz). HRMS (ESI): calcd for $C_{18}H_{10}F_2N_2O_2$ $[M+H]^+$ 325.0783, found 325.0775. HPLC purity: 99.9%.

1-Methyl-2-(2,3,4-trifluorophenyl)-1*H*-perimidine-7,8-dione (**a-17**): Red solid, Yield 24%. ^{1}H NMR (400 MHz, DMSO) δ 8.10 (d, J = 6.4 Hz, 1H), 8.01–7.79 (m, 2H), 7.61 (m, 2H), 5.94 (s, 1H), 3.40 (s, 3H). ^{13}C NMR (101 MHz, $CDCl_3$) δ 179.7, 177.8, 154.4–154.1 (m), 152.1–151.4 (m), 151.3, 149.8 (d, J = 2.7 Hz), 148.0–147.4 (m), 141.6 (d, J = 3.7 Hz), 135.0, 133.4, 131.4, 129.5, 124.7, 120.9–119.6 (m), 118.4, 114.0 (dd, J = 17.7, 2.1 Hz), 100.8, 37.5. HRMS (ESI): calcd for $C_{18}H_{19}F_3N_2O_2$ $[M+H]^+$ 343.0689, found 343.0682. HPLC purity: 100%.

1-Methyl-2-(2,3,4-trifluorophenyl)-1*H*-perimidine-5,6-dione (**b-17**): Purple solid, Yield 17.4%. ^{1}H NMR (400 MHz, DMSO) δ 8.09–8.00 (m, 2H), 7.90 (dd, J = 8.6, 7.4 Hz, 1H), 7.71–7.46 (m, 2H), 5.85 (s, 1H), 3.62 (s, 3H). ^{13}C NMR (101 MHz, TFA) δ 174.4 (2C), 160.5, 159.3, 153.7, 151.2 (dddd, J = 263.0, 10.2, 3.8, 2 Hz), 145.3 (dddd, J = 258.2, 12.0, 4.1, 2 Hz), 134.6 (2C), 134.5, 130.0 (2C), 123.2, 122.0–120.8 (m), 112.8, 110.4 (dd, J = 19.0, 3.1 Hz), 106.0, 35.8 (d, J = 4.9 Hz). HRMS (ESI): calcd for $C_{18}H_{19}F_3N_2O_2$ $[M+H]^+$ 343.0689, found 343.0684. HPLC purity: 100%.

*5.5. Procedure for the preparation of 9-chloro-2-(2-chlorophenyl)-1-methyl-1H-perimidine-7,8-dione (**d-2**)*

N-Chlorosuccinimide (0.6 mmol, 1.2 equiv.) and benzoyl peroxide (12 mg) were added to a solution of *o*-quinone products (0.5 mmol) in

chloroform. The reaction mixture was stirred at 80 °C. After the reaction was completed, the chloroform was evaporated. The residue was used for futher purification to obtain the red product. Red solid, Yield 63%. ^{1}H NMR (400 MHz, $CDCl_3$) δ 8.23 (d, J = 7.2 Hz, 1H), 7.89 (d, J = 7.9 Hz, 1H), 7.73 (t, J = 7.6 Hz, 1H), 7.63 (t, J = 8.6 Hz, 1H), 7.61–7.45 (m, 3H), 3.73 (s, 3H). ^{13}C NMR (101 MHz, $CDCl_3$) δ 178.0, 173.7, 155.4, 150.0, 141.5, 135.3, 133.5, 132.9, 132.6, 132.3, 131.5, 130.7, 130.6, 128.0, 127.7, 119.6, 108.4, 43.7. HRMS (ESI): calcd for $C_{18}H_{10}Cl_2N_2O_2$ $[M+H]^+$ 357.0192, found 357.0191. HPLC purity: 97.9%.

5.6. General procedure for the preparation of **d-1** and **d-3**

N-Bromosuccinimide (0.6 mmol, 1.2 equiv.) and benzoyl peroxide (12 mg) were added to a solution of *o*-quinone products (0.5 mmol) in chloroform. The reaction mixture was stirred at 80 °C. After the reaction was completed, the chloroform was evaporated. The residue was used for futher purification to obtain the red product.

9-Bromo-2-(2-chlorophenyl)-1-methyl-1*H*-perimidine-7,8-dione (**d-1**): Red solid, Yield 71%. ^{1}H NMR (400 MHz, $CDCl_3$) δ 8.21 (d, J = 7.4 Hz, 1H), 7.89 (d, J = 8.1 Hz, 1H), 7.73 (t, J = 7.7 Hz, 1H), 7.66 (d, J = 6.9 Hz, 1H), 7.62–7.46 (m, 3H), 3.74 (d, J = 5.9 Hz, 3H). ^{13}C NMR (101 MHz, $CDCl_3$) δ 177.5, 173.9, 155.4, 152.5, 141.3, 135.2, 133.5, 132.9, 132.6, 132.3, 131.3, 130.9, 130.6, 128.0, 127.7, 120.5, 98.2, 44.5. HRMS (ESI): calcd for $C_{18}H_{10}ClBrN_2O_2$ $[M+H]^+$ 400.9687, found 400.9683. HPLC purity: 97.8%.

9-Bromo-2-ethyl-1-methyl-1*H*-perimidine-7,8-dione (**d-3**): Red solid, Yield 77.5%. ^{1}H NMR (400 MHz, $CDCl_3$) δ 8.12 (d, J = 7.4 Hz, 1H), 7.79 (d, J = 8.0 Hz, 1H), 7.67 (t, J = 7.7 Hz, 1H), 3.91 (s, 3H), 2.89 (q, J = 7.3 Hz, 2H), 1.44 (t, J = 7.3 Hz, 3H). ^{13}C NMR (101 MHz, $CDCl_3$) δ 177.8, 173.9, 159.7, 153.2, 141.2, 134.6, 132.7, 130.5, 127.5, 120.0, 97.0, 42.7, 28.5, 11.1. HRMS (ESI): calcd for $C_{14}H_{11}BrN_2O_2$ $[M+H]^+$ 319.0077, found 319.0073. HPLC purity: 98.7%.

5.7. Topo I mediated DNA relaxation assay

The effects of compounds on DNA relaxation catalyzed by DNA Topo I (TaKaRa, Kyoto, Japan) were determined by measuring the relaxation of supercoiled DNA pBR322 (TaKaRa, Kyoto, Japan) using CPT as the positive control. The reaction solution was prepared according to the provided protocol and incubated at 37 °C for 30 min. The reactions were stoped by the 6 × loading buffer (provided by TaKaRa) of 4 μL. The products were applied to 1% agarose gel and subjected to electrophoresis for 1.5 h at 100 V in 1 × TAE buffer (40 mM Tris-acetate, 2 mM EDTA). Gels were stained for 30 min in 30 mL 1 × TAE buffer with 1 μL Gel Red. DNA bands were visualized by transillumination with UV light and then photographed by Alpha Innotech digital imaging system.

5.8. Topo IIα mediated DNA relaxation assay

We used the Topo IIα assay kit from TopoGEN to determine the effects of compounds on DNA relaxation catalyzed by Topo II. Relaxation assays were carried out according to the manufacturer's instructions with minor modifications. The assay was performed in a final volume of 20 μL in Topo II reaction buffer (5 × Topo II buffer = 50 mM Trise HCl, pH 8.0, 150 mM NaCl, 10 mM $MgCl_2$ 2 mM ATP, 0.5 mM dithiothreitol, and 30 μg/mL BSA) with 0.2 μg pBR322 DNA. Then reactions were initiated by 1U human Topo IIα and incubated for 30 min at 37 °C. Finally reaction was stoped with the 6 × loading buffer of 4 μL. Reaction products were analyzed on a 1% agarose gel in 1 × TAE buffer. Gels were stained for 30 min in 30 mL 1 × TAE buffer with 1 μL Gel Red. DNA bands were visualized through transillumination with UV light and then photographed by Alpha Innotech digital imaging system.

5.9. Topo I mediated DNA cleavage assay

In brief, Topo I (10 U), supercoiled pBR322 DNA (0.1 μg) and compounds (different concentrations) were added in Topo I buffer (50 mM Trise-HCl, pH 7.5, 50 mM KCl, 10 mM $MgCl_2$, 0.5 mM DTT, 0.1 mM EDTA and 30 μg/mL bovine serum albumin, provided by TaKaRa) of 20 μLvolume. After incubating for 6 min at 37 °C and then respectively adding 2 μL of 10% SDS, 2 μL of 250 mM NaEDTA, pH 8.0, 2 μL of 0.8 mg/mL Proteinase K. Following reactions were incubated for another 30 min at 45 °C. Samples were mixed with 4 μL of 6 × loading buffer, heated at 70 °C for 2 min and subjected to electrophoresis in a 1% agarose gel in 1 × TAE buffer (30 mL) with 1 μL Gel Red. Finally DNA bands were visualized by using UV light, photographed by using Alpha Innotech digital imaging system.

5.10. Topo II mediated DNA cleavage assay

In brief, Topo IIα (10 U), supercoiled pBR322 DNA (0.2 μg) and compounds (different concentrations) were added in Topo II buffer (5 × Topo II buffer = 50 mM Trise HCl, pH 8.0, 150 mM NaCl, 10 mM $MgCl_2$ 2 mM ATP, 0.5 mM dithiothreitol, and 30 μg/mL BSA) of 20 μL volume. The following procedure was same with that Topo I mediated DNA cleavage Assay. Finally DNA bands were visualized by using UV light, photographed by using Alpha Innotech digital imaging system.

5.11. DNA unwinding assays

The ability of perimidine derivatives to unwind plasmid DNA was determined as described by Fortune et al with modifications. The relaxed pBR322 plasmid DNA utilized in unwinding assays was generated by treating negatively supercoiled pBR322 with Topo I in Topo I reaction buffer at 37 °C for 30 min. Reactions included 0.1 μg relaxed pBR322 plasmid DNA and different concentrations compounds in 20 μL of Topo I reaction buffer were incubated for 10 min in room temperature. Then Topo I was added and reactions were incubated for another 30 min at 37 °C. Finally, reactions were stoped by 4 μL of 6 × loading buffer, subjected to electrophoresis in a 1% agarose gel in 1 × TAE buffer (30 mL) with 1 μL Gel Red And DNA bands were visualized by using UV light, photographed by using Alpha Innotech digital imaging system.

5.12. UV–Vis titration assay

Absorbance titration experiments were performed as previously described [21]. A solution of CT-DNA (Sigma-Aldrich) in DPBS gave a ratio of UV–Vis absorbance of 1.8–1.9 at 260 and 280 nm, indicating that the DNA was sufficiently free of protein. The CT-DNA concentration was determined by UV absorbance at 260 nm using a molar absorptivity constant of 6600 M^{-1} cm^{-1}

Compound **b-12** (5 μM) was prepared in DPBS in the presence or absence of increasing concentrations of CT-DNA (0–80 μM). Absorption spectra were recorded in the 450–650 nm spectral range after equilibration at room temperature for 5 min using UV evisible spectrophotometer UV-2450 (Shimadzu Instruments, Inc.).

5.13. MTT assay

The growth inhibitory effects of perimidine derivatives against four cancer cell lines were evaluated by using the MTT assay as described by Mosmann with modifications [22]. The cells were plated at a density of 5000 per well in 96-well microplates and allowed to incubate for 24 h at 37 °C. Compounds were added to the wells at different concentrations and incubated for 48 h at 37 °C. To adherent cells, each well was treated with 20 μL of 2.5 mg/mL MTT solution and incubated for 4 h, and finally 100 mL of DMSO was added. The microplates were well shaken to dissolve the formazan dye, and the absorbance at 570 nm was measured

using a microplate reader (Bio-Tek). All compound doses were parallel tested in triplicate.

5.14. Cell apoptosis assay

Huh7 cells (5×10^5 cells per mL) were incubated in the presence of compound for 24 h at 37 °C, then harvested and washed twice with cold 1 × PBS, resuspended in 1 × binding buffer, and then stained with 5 μL of Fluorescein isothiocyanate (FITC) Annexin V and 5 μL of propidium iodide (KeyGEN BioTECH, China) for 15 min in the dark. The stained cells were analyzed by flow cytometry (BD, FACSCalibur, USA) within 1 h.

5.15. Cell cycle assay

Huh7 cells (5×10^5 cells per mL) were incubated in the presence of compound for 24 h at 37 °C, then harvested and washed twice with cold 1 × PBS, resuspended in 1 × binding buffer, and then stained with 500 μL of propidium iodide (KeyGEN BioTECH, China) for 15 min in the dark. The stained cells were analyzed by flow cytometry (BD, FACSCalibur, USA) within 1 h.

5.16. Immunofluorescence assay

Huh7 Cells grown on glass coverslips were fixed in 4% paraformaldehyde/PBS for 15 min, then permeabilized with 0.5% triton-X100/PBS at 37 °C for 30 min, and finally blocked with 5% goat serum/PBS at 37 °C for 2 h. Immunofluorescence was performed using standard methods, and the slides were incubated alternately with Phospho-γH_2AX(Ser139) (Cell Signaling Technology) at 37 °C for 2 h. the glass coverslips were washed six times with blocking buffer and were then incubated with ant-rabbit Alexa 488-conjugated antibody (A21206, Life Technology), and 2 μg/mL of 4′,6-diamidino-2-phenylindole (DAPI, Invitrogen) at 37 °C for 3 h. The glass coverslips were again washed six times with blocking buffer. Digital images were recorded using an LSM710 microscope (Zeiss, GER) and analyzed with ZEN software.

Acknowledgements

We thank the Guangdong Provincial Key Laboratory of Construction Foundation [2017B030314030] for financial support of this study. We also thank Professor Jian Ding and Hong Liu (State Key Laboratory of Drug Research, Shanghai Institute of Materia Medica, Chinese Academy of Sciences) for the HL-60/MX2 cell line gifts.

Appendix A. Supplementary material

Supplementary data to this article can be found online at https://doi.org/10.1016/j.bioorg.2019.103131.

References

[1] J.J. Champoux, DNA topoisomerases: structure, function, and mechanism, Annu. Rev. Biochem. 70 (2001) 369–413.
[2] A.K. Larsen, A.E. Escargueil, A. Skladanowski, Catalytic topoisomerase II inhibitors in cancer therapy, Pharmacol. Ther. 99 (2) (2003) 167–181.
[3] P.B. Jensen, P.S. Jensen, E.J. Demant, E. Friche, B.S. Sorensen, M. Sehested, K. Wassermann, L. Vindelov, O. Westergaard, H.H. Hansen, Antagonistic effect of aclarubicin on daunorubicin-induced cytotoxicity in human small cell lung cancer cells: relationship to DNA integrity and topoisomerase II, Cancer Res. 51 (19) (1991) 5093–5099.
[4] M. Lehmann, S. Vilar Kde, A. Franco, M.L. Reguly, H.H. Rodrigues de Andrade, Activity of topoisomerase inhibitors daunorubicin, idarubicin, and aclarubicin in the Drosophila Somatic Mutation and Recombination Test, Environ. Mol. Mutagen. 43 (4) (2004) 250–257.
[5] S.E. Morgan, R.S. Cadena, S.C. Raimondi, W.T. Beck, Selection of human leukemic CEM cells for resistance to the DNA topoisomerase II catalytic inhibitor ICRF-187 results in increased levels of topoisomerase IIalpha and altered G(2)/M checkpoint and apoptotic responses, Mol. Pharmacol. 57 (2) (2000) 296–307.
[6] A.K. McClendon, N. Osheroff, DNA topoisomerase II, genotoxicity, and cancer, Mutat. Res. 623 (1–2) (2007) 83–97.
[7] F.M. Kalfalah, C. Mielke, M.O. Christensen, S. Baechler, D. Marko, F. Boege, Genotoxicity of dietary, environmental and therapeutic topoisomerase II poisons is uniformly correlated to prolongation of enzyme DNA residence, Mol. Nutr. Food Res. 55 (Suppl 1) (2011) S127–S142.
[8] J.S. Driscoll, G.F. Hazard Jr., H.B. Wood Jr., A. Goldin, Structure-antitumor activity relationships among quinone derivatives, Cancer Chemother. Rep. Part 2 4 (2) (1974) 1–362.
[9] Y.J. Cai, J.J. Lu, H. Zhu, H. Xie, M. Huang, L.P. Lin, X.W. Zhang, J. Ding, Salvicine triggers DNA double-strand breaks and apoptosis by GSH-depletion-driven H2O2 generation and topoisomerase II inhibition, Free Radic. Biol. Med. 45 (5) (2008) 627–635.
[10] B.S. Kumar, K. Ravi, A.K. Verma, K. Fatima, M. Hasanain, A. Singh, J. Sarkar, S. Luqman, D. Chanda, A.S. Negi, Synthesis of pharmacologically important naphthoquinones and anticancer activity of 2-benzyllawsone through DNA topoisomerase-II inhibition, Bioorg. Med. Chem. 25 (4) (2017) 1364–1373.
[11] D. Wang, M. Xia, Z. Cui, S. Tashiro, S. Onodera, T. Ikejima, Cytotoxic effects of mansonone E and F isolated from Ulmus pumila, Biol. Pharm. Bull. 27 (7) (2004) 1025–1030.
[12] M.F. Brana, M. Garrido, M. Lopez Rodriguez, M.J. Morcillo, Y. Alvarez, Y. Valladares, G. Klebe, Synthesis, structure and cytostatic activity of a series of 2-substituted perimidines, Eur. J. Med. Chem. 25 (1990) 209–215.
[13] T.A. Farghaly, H.K. Mahmoud, Synthesis, tautomeric structures, and antitumor activity of new perimidines, Arch. Pharm. (Weinheim) 346 (5) (2013) 392–402.
[14] M. Dzieduszycka, S. Martelli, M. Arciemiuk, M.M. Bontemps-Gracz, A. Kupiec, E. Borowski, Effect of modification of 6-[(aminoalkyl)amino]-7H-benzo[e]-perimidin-7-ones on their cytotoxic activity toward sensitive and multidrug resistant tumor cell lines. Synthesis and biological evaluation, Bioorg. Med. Chem. 10 (4) (2002) 1025–1035.
[15] J.J. Vandeneynde, A. Mayence, A. Maquestiau, E. Anders, Novel syntheses of heterocycles with N-(1-haloalkyl)azinium halides. Part 4. An unexpected one-pot preparation of 1H-perimidines, Synthetic Commun. 22 (21) (2009) 3141–3150.
[16] B.S. Glisson, S.E. Smallwood, W.E. Ross, Characterization of VP-16-induced DNA damage in isolated nuclei from L1210 cells, Biochim. Biophys. Acta 783 (1) (1984) 74–79.
[17] K. Tanabe, Y. Ikegami, R. Ishida, T. Andoh, Inhibition of topoisomerase II by antitumor agents bis(2,6-dioxopiperazine) derivatives, Cancer Res. 51 (18) (1991) 4903–4908.
[18] P. Rybak, A. Hoang, L. Bujnowicz, T. Bernas, K. Berniak, M. Zarebski, Z. Darzynkiewicz, J. Dobrucki, Low level phosphorylation of histone H2AX on serine 139 (gammaH2AX) is not associated with DNA double-strand breaks, Oncotarget 7 (31) (2016) 49574–49587.
[19] S. Park, E. Hong, S.Y. Kwak, K.Y. Jun, E.S. Lee, Y. Kwon, Y. Na, Synthesis and biological evaluation of C1-O-substituted-3-(3-butylamino-2-hydroxy-propoxy)-xanthen-9-one as topoisomerase IIalpha catalytic inhibitors, Eur. J. Med. Chem. 123 (2016) 211–225.
[20] J.E. Deweese, N. Osheroff, The DNA cleavage reaction of topoisomerase II: wolf in sheep's clothing, Nucl. Acids Res. 37 (3) (2009) 738–748.
[21] G. Dong, S. Wang, Z. Miao, J. Yao, Y. Zhang, Z. Guo, W. Zhang, C. Sheng, New tricks for an old natural product: discovery of highly potent evodiamine derivatives as novel antitumor agents by systemic structure-activity relationship analysis and biological evaluations, J. Med. Chem. 55 (17) (2012) 7593–7613.
[22] T. Mosmann, Rapid colorimetric assay for cellular growth and survival: application to proliferation and cytotoxicity assays, J. Immunol. Methods 65 (1–2) (1983) 55–63.